INTERDIGITATED BACK CONTACT SILICON SOLAR CELLS FEATURING ION-IMPLANTED POLY-SI/SIOX PASSIVATING CONTACTS

Christian Reichel[1], Ralph Müller[1,2], Frank Feldmann[1,2], Armin Richter[1], Martin Hermle[1], Stefan W. Glunz[1,2]
[1]Fraunhofer Institute for Solar Energy Systems (ISE), Heidenhofstrasse 2, 79110 Freiburg, Germany
[2]Department of Sustainable Systems Engineering (INATECH), Albert Ludwigs University Freiburg, Georges-Köhler-Allee 103, 79110 Freiburg, Germany

ABSTRACT: Interdigitated back contact (IBC) silicon solar cells featuring passivating contacts based on tunneling oxides (SiO_x) and n- and p-type polycrystalline silicon (poly-Si) thin films were fabricated with different rear side configurations to show the impact of the recombination in the transition region between p-type and n-type poly-Si on the performance of the solar cells. On the one hand a) p^+ and n^+ poly-Si regions were in direct contact to each other (“no gap”) using a local overcompensation (counterdoping) as a self-aligning process and on the other hand b) undoped (intrinsic) poly-Si remained between the p^+ and n^+ poly-Si regions (“gap”). These configurations were investigated in terms of recombination characteristics by illumination- and injection-dependent quasi-steady state photoluminescence (suns-PL) and were compared to solar cells that featured c) etched trenches separating the p^+ and n^+ poly-Si regions (“trench”). While the latter configuration allowed for open-circuit voltages (V_{oc}) of 720 mV, fill factor (FF) of 79.6%, and short-circuit current (J_{sc}) of 41.3 mA/cm^2, resulting in conversion efficiencies (η) of 23.7%, solar cells without a trench showed a poor performance due to non-ideal recombination in the space charge regions with high local ideality factors as well as recombination in shunted regions. Therefore, V_{oc} of only 593 mV and FF of only 61.3% were achieved for the “no gap” configuration whereas for the “gap” configuration higher V_{oc} of 680 mV but also low FF of 65.6% were obtained.

Keywords: amorphous silicon, annealing, back contact, deposition, heterojunction, lifetime, passivation, polycrystalline, recombination, solar cells

1 INTRODUCTION

Interdigitated back contact (IBC) silicon solar cells featuring passivating contacts have pathed the way to efficiencies of more than 25% as presented by SunPower [1], Sharp [2] and Panasonic [3]. Kaneka pushed the limits even further and achieved a world record of 26.7% utilizing intrinsic and doped amorphous silicon (a-Si) thin films as passivating contacts with excellent passivation and excellent transport properties [4,5]. These excellent properties are currently challenged by another passivating contact based on semicrystalline or polycrystalline silicon (poly-Si) and silicon oxide (SiO_x) thin films, named tunnel oxide passivated contacts (TOPCon) or polycrystalline silicon on oxide (POLO) contacts which gained a lot of interest in the past years and re-emerged as a competitive and alternative technology to a-Si thin films [6,7]. The application of poly-Si thin films resulted in efficiencies of up to 25.7%, realized on n-type c-Si with a p-type boron-diffused emitter on the front and a n-type poly-Si thin film as a passivating contact. In fact, this represents the highest efficiency reported for both-sides contacted c-Si solar cells, allowing open-circuit-voltages (V_{oc}) of 725 mV and fill factors (FF) of 83.3%[6].

The integration of these poly-Si thin films into single-side contacted c-Si solar cells however poses a challenge due to high recombination in the transition from p- to n-type poly-Si [8–12]. This was first shown by SunPower in 2009 [8] and later encountered by several other groups [9–12]. In order to show the effects of the recombination on the performance of the solar cells in more detail, the transition region between p-type and n-type poly-Si was created in different configurations. On the one hand a) p^+ and n^+ poly-Si regions were in direct contact to each other (“no gap”) using a local overcompensation (counterdoping) as a self-aligning process [9,10] and on the other hand b) undoped (intrinsic) poly-Si remained between the p^+ and n^+ poly-Si regions (“gap”) [13]. These configurations were compared to solar cells that featured c) etched trenches separating the p^+ and n^+ poly-Si regions (“trench”) [7,12,14], see Figure 1. With illumination- and injection-dependent quasi-steady state photoluminescence (suns-PL) measurements the charge carrier lifetime and open-circuit voltage characteristic of the solar cells were determined. In this respect, the open-circuit voltage characteristics of the solar cells were modeled to reveal the dominating recombination mechanism that is influencing the performance of the solar cells.

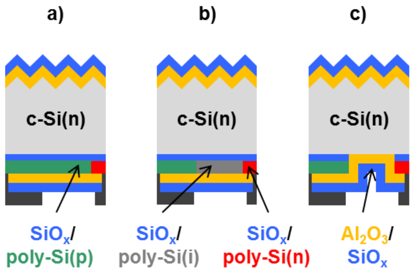

Figure 1: Schematic illustration of the solar cells with different configurations: a) p^+ and n^+ poly-Si regions in direct contact to each other (“no gap”), b) undoped (intrinsic) poly-Si remains between p^+ and n^+ poly-Si regions (“gap”) and c) trenches separate p^+ and n^+ poly-Si regions.

2 EXPERIMENTAL

IBC solar cells with an area of 2 cm × 2 cm were fabricated on shiny-etched <100>-oriented phosphorus (P)-doped n-type float-zone silicon wafers with a specific resistivity of 1 Ωcm and a thickness of 200 µm. The front side was textured with random pyramids. Then an ultra-thin tunneling silicon oxide (SiO_x), about 1.5 nm, was wet-chemically grown [15]. Subsequently, about 35 nm of intrinsic amorphous silicon (a-Si) was deposited on the wafers by low-pressure chemical vapor deposition (LPCVD) [16]. Boron monofluoride (BF) ions were then introduced into the intrinsic a-Si by ion implantation at an ion dose of 5×10^{14} cm^{-2} either on the entire rear side for the “no gap” configuration or locally via a SiO_x mask for the “gap” configuration. P ions were then implanted via another SiO_x mask either into the intrinsic a-Si at an ion dose of 1.5×10^{15} cm^{-2} for the “gap” configuration or into the boron-doped a-Si at an ion dose of 2.3×10^{15} cm^{-2} for the “no gap” configuration as a counterdoping process [17], applying an ion energy of 2 keV [18]. The pitch distance of the IBC solar cells was 500 µm, whereas for the “no gap” (“gap”) configuration the emitter was 400 µm (360 µm) and the BSF was 100 µm wide. In the “gap” configuration, a 20 µm wide undoped (intrinsic) a-Si remained between the doped a-Si. For the fabrication of the solar cells with a trench, some of the solar cells with the undoped (intrinsic) a-Si, the a-Si was dry-chemically etched via a sacrificial SiO_x mask, creating a 20 µm wide trench. Afterwards, a high-temperature anneal was conducted, transforming the a-Si into poly-Si. BF- and P-implantations resulted in sheet resistances of about 1000 Ω/sq as measured for the whole stack with constant doping densities of about 3.0×10^{19} cm^{-3} in the poly-Si and a shallow doping tail extending to about 50 nm into c-Si. Then a 10 nm aluminum oxide (Al_2O_3) was deposited on both sides, succeeded by a 60 nm silicon nitride (SiN_x) antireflection coating deposition [19] on the front side and a 100 nm SiO_x deposition on the rear side. Afterwards, a hydrogen passivation was applied in a remote-plasma hydrogen passivation (RPHP) system [20]. Prior to the thermal evaporation and the lift-off of several 10 µm wide and in total 100 nm thick titanium (Ti) and palladium (Pd) lines, local openings were etched in Al_2O_3 and SiO_x on the rear. Finally, 5 µm thick aluminum (Al) was thermally evaporated and locally to realize the finger grid and the busbars in an interdigitated pattern. Photolithography was used for the several patterning processes and the lift-off. Additionally, asymmetric control samples with the same front side as the solar cells, but different rear sides (poly-Si(p), poly-Si(n) and poly-Si(i) as well as Al_2O_3/SiO_x) were fabricated using the same processes as described above

The current-voltage (IV) parameters of the solar cells were measured under standard testing conditions (STC). and, furthermore, in forward and in reverse direction without illumination. In addition, the illumination- and injection-dependent charge carrier lifetime characteristics were determined for the solar cells using quasi-steady state photoluminescence (suns-PL) measurements [21,22] and for the asymmetric control samples transient photoconductance decay measurements were performed [23,24]. In this way, effective minority charge carrier lifetimes (τ_{eff}) and implied open-circuit voltages (iV_{oc}), equivalent to the quasi-Fermi level splitting in the silicon volume at an injection level corresponding to open-circuit (OC) conditions, and implied fill factors (iFF) at an injection level corresponding to maximum power point (MPP) conditions were obtained. For the asymmetric control samples, iV_{oc} was used to determine the surface saturation current density (J_{0s}) of the different rear sides. Furthermore, illumination- and injection-dependent quasi-steady state open-circuit voltage (suns-V_{oc}) curves of the solar cells were measured to determine the series resistance (R_s) of the solar cells, calculating R_s from the difference in pFF and FF [25].

3 RESULTS

Table 1 presents the results of the different solar cell configurations. The solar cells without a trench showed a poor performance due to detrimental recombination in the transition region between p-type and n-type poly-Si. This is in good accordance with the observations for lateral poly-Si pn- and pin-diodes where defects at grain boundaries greatly enhanced the recombination [26–28]. The detrimental recombination was even more pronounced for the “no gap” configuration, allowing V_{oc} and FF of only 593 mV and 61.3%, respectively. For the “gap” configuration, V_{oc} of up to 680 mV and FF of 65.6% were obtained. In this case, R_s was twice as high as for the “no gap” configuration. For both configurations additional junction and/or shunt leakage currents were observed when measuring the non-illuminated IV curves which limit the V_{oc} and FF of the solar cells. In contrast, solar cells with trenches allowed for V_{oc} of 720 mV, FF of 79.6% and J_{sc} of 41.3 mA/cm^2, resulting in η of 23.7%.

Table I: IV and suns-PL parameters of the IBC solar cells with different configurations, showing the best values measured under standard testing conditions (AM1.5G, 100 mW/cm^2, 25 °C) for a designated area of 4.0 cm^2.

V_{oc} (mV)	J_{sc} (mA/cm^2)	FF (%)	iV_{oc} (mV)	iFF (%)	R_s (Ωcm^2)	η (%)
a) “no gap” configuration						
593	41.5	61.3	597	62.7	0.38	15.1
b) “gap” configuration						
680	41.2	65.6	675	68.8	0.67	18.4
c) “trench” configuration						
720*	41.3*	79.6*	724	81.2	0.34	23.7*

* independently confirmed by Fraunhofer ISE CalLab

The V_{oc}-limit of the solar cells was calculated, based on an ideal saturation current density (J_{01}) as a sum of the area-weighted surface and bulk saturation current density (J_{0s}) and (J_{0b}), respectively, of the asymmetrical control samples. J_{0b} was around 8 fA/cm^2 and J_{0s} was around 3 fA/cm^2 for the Al_2O_3/SiN_x on the textured front side of the wafer. J_{0s} of the poly-Si(p) and poly-Si(n) was 11 fA/cm^2 and 5 fA/cm^2, respectively, whereas Al_2O_3/SiO_x on the rear side of the wafer allowed for 2 fA/cm^2. The intrinsic the poly-Si(i) thin film has a much higher recombination, resulting in J_{01} of 78 fA/cm^2. J_{0b} was calculated using the experimentally determined charge carrier lifetime of 7.2 ms for symmetrical lifetime samples [29] with an intrinsic carrier concentration n_i of 8.79×10^9 cm^{-3} at 25°C.

Using these values for the “trench” configuration, the V_{oc}-limit was 724 mV (J_{01} of 21 fA/cm^2). For the “no gap” and the “gap” configuration, the V_{oc}-limit was 723 mV (J_{01} of 22 fA/cm^2) and 718 mV (J_{01} of 28 fA/cm^2), respectively. In the latter case, the V_{oc}-limit is much higher than the actual measured V_{oc} of the solar cells. Thus, the transition region which is not accounted for in this simple evaluation , has a strong impact on the recombination behavior of the cell. .

In order to evaluate the impact of the recombination in the transition region on the performance of the solar cells, iV_{oc} and iFF on finished solar cells were additionally determined by suns-PL measurements. In this case, iV_{oc} is a measure of the splitting of the quasi-Fermi levels of the minority charge carriers which is affected by recombination in the silicon volume and at all surfaces or interfaces, and can be calculated by measuring the average excess carrier density (Δn_{av}) of the solar cells [23,24]. In order to account for diffusion limited lifetime carriers [30], the injection-dependent charge carrier lifetime characteristics of the solar cells were additionally determined under short-circuit (SC) conditions performing suns-PL measurements with the same generation [31]. Subtracting Δn_{av} under SC conditions from Δn_{av} under OC conditions leads to Δn_{av} at the junction of the solar cells so that iV_{oc} and iFF can be extracted from the corrected suns-PL measurements, see Figure 2. The illumination-dependent iV_{oc} curves of the solar cells were then modeled to analyze the origin of the recombination in the transition region. In this case, the injection-dependent charge carrier lifetime characteristics was calculated, using radiative, Auger [32], bulk and surface recombination [33] as well as recombination in space-charge regions and in shunted regions [34], and converted into illumination-dependent iV_{oc} curves. The resulting illumination-dependent iV_{oc} curves were then interpreted in terms of the dominating recombination mechanisms [35].

For the “no gap” configuration, the illumination-dependent iV_{oc} curves from the corrected suns-PL measurements are marked by low iV_{oc} values due to detrimental recombination. Since high-quality silicon wafers were used and since the front surfaces as well as the p^+ and n^+ poly-Si rear surfaces enable high minority charge carrier lifetimes of more than several milliseconds, most of the recombination originates from the recombination in the transition region from the p^+ to the n^+ poly-Si. In this respect, J_{01} of 21 fA/cm^2 was used for the bulk and surface recombination, see Figure 2a (green curve), but additional recombination terms were required to obtain a good fit at moderate and low illumination intensities. At these illumination intensities, recombination in space-charge regions and in shunted regions can occur. Therefore, a saturation current density (J_{scr}) of 17000 nA/cm^2 was used with a local ideality factor of 3.0, for the space-charge regions and a R_{sh} of 0.5 kΩcm^2 was used for the shunted regions, see Figure 2a (orange and brown curve). The high local ideality factors indicate that non-ideal recombination in the space charge regions of these solar cells exists [10,12,13] which limit the iV_{oc} to 597 mV and the iFF to 62.7%. Local ideality factors of 3.0 were also reported for lifetime samples with a direct contact of p^+ and n^+ poly Si regions [10]. Hence, it can be concluded that for the “no gap” configuration non-ideal recombination in the space charge regions as well as recombination in shunted regions are the limiting factors allowing V_{oc} to only 593 mV and FF of only 61.3% for these solar cells.

In comparison, the illumination-dependent iV_{oc} curves of the “gap” configuration shows a different behavior. Here, higher iV_{oc} values were obtained. J_{01} of 28 fA/cm^2 was used for bulk and surface recombination, see Figure 2b (green curve). For the space-charge region recombination, J_{scr} of 3600 nA/cm^2 was used with a local ideality factor of 2.9, whereas for recombination in the shunted region an R_{sh} of 0.57 kΩcm^2 was used to obtain a good fit at moderate and low illumination intensities, see Figure 2b (orange and brown curve).

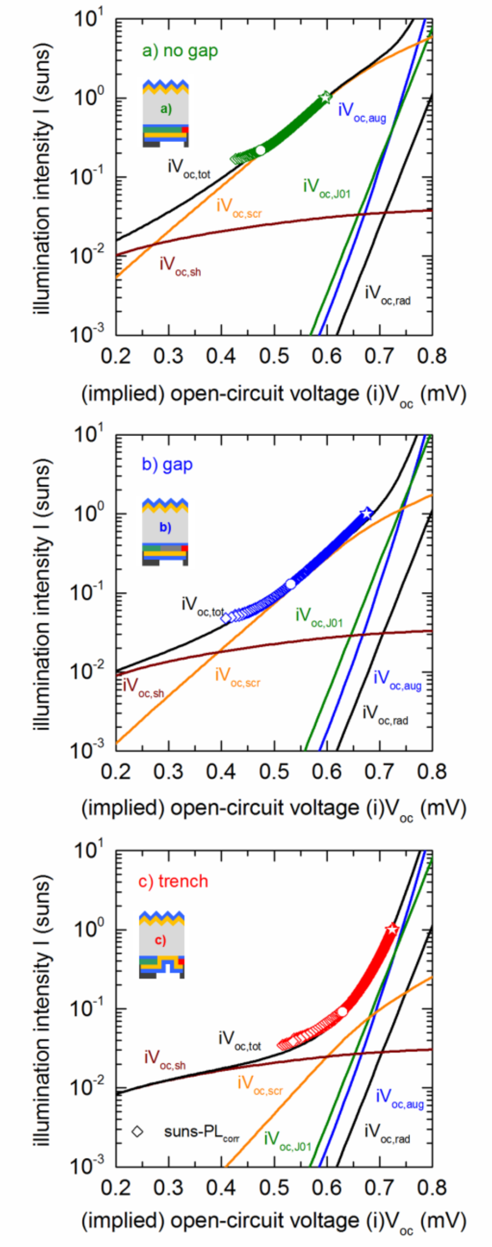

Figure 2: Illumination intensity (I) vs. (implied) open-circuit voltage $(i)V_{oc}$ from corrected suns-PL measurements under open-circuit (OC) conditions of the different solar cell configurations: a) no gap, b) gap and c) trench (schematic illustration, insets). Stars and circles denote the position corresponding to OC and to maximum power point (MPP) conditions, respectively. Radiative (black), Auger (blue), bulk and surface recombination (green) as well as recombination in space-charge regions (orange) and shunted regions (brown) are modeled.

In this case, the local ideality factors are almost in the same range as compared to the “no gap” configuration and also indicate that non-ideal recombination in the space charge regions of these solar cells exists which limit the iV_{oc} to 680 mV and the iFF to 68.7%.

In contrast to solar cells without a trench, the illumination-dependent iV_{oc} curves of the “trench” configuration shows a completely different behavior. At high illumination intensities Auger and rear surface recombination dominate, whereas at moderate and low illumination intensities recombination in the space-charge region and in shunted regions dominate. For the rear surface recombination, J_{01} was 21 fA/cm^2, see Figure 2c (green curve), whereas for the space-charge region recombination, J_{scr} was 40 nA/cm^2 when a local ideality factor of 2.3 was used and for recombination in the shunted region, R_{sh} was 0.62 kΩcm^2, see Figure 2c (orange and brown curve). The local ideality factors are much lower as compared to solar cells without a trench, indicating a more ideal recombination behavior for the “trench” configuration. Therefore, high iV_{oc} of 724 mV and high iFF of 81.2% were achieved. However, even here additional junction and/or shunt leakage currents were observed but to a much lesser extent, limiting the iFF and thus the FF of these solar cells. In this respect, the influence of shunts due to locally etched poly-Si (defects in the sacrificial SiO_x mask) and/or of junction leakage currents due to the inversion layer in the trench (presence of Al_2O_3 passivation) have to be examined in the future.

4 SUMMARY AND CONCLUSIONS

In summary, the recombination within the highly-defective poly-Si is detrimental for the performance of interdigitated back contact (IBC) silicon solar cells where the p^+ and n^+ poly-Si regions are in direct contact to each other and where undoped (intrinsic) poly-Si remains between the p^+ and n^+ poly-Si regions. Illumination- and injection-dependent quasi-steady state photo-luminescence (suns-PL) measurements revealed that non-ideal recombination in the space charge regions, characterized by high local ideality factors, as well as recombination in shunted regions is dominating the recombination behavior. While for the “pn-junction” configuration, the highest junction leakage currents and lowest shunts resistances were determined, it was observed that intrinsic poly-Si between the p^+ and n^+ poly-Si regions increased the shunt resistance slightly but could not prevent the detrimental recombination in the space charge region. In contrast, the separation of the p^+ and n^+ poly-Si regions by a trench enabled highly efficient solar cells (V_{oc} of 720 mV, FF of 79.6%, J_{sc} of 41.3 mA/cm^2, η of 23.7%), showing that a lowly conducting and highly passivating intermediate layer is mandatory between the p^+ and n^+ poly-Si regions of IBC solar cells with poly-Si passivating contacts.

5 ACKNOWLEDGEMENTS

The authors would like to thank A. Leimenstoll, F. Schätzle, S. Seitz, A. Seiler, A. Lösel, E. Schäffer, and F. Martin for preparation and measurements of the solar cells. The authors also acknowledge M. Bauer from the Department of Microsystems Engineering (IMTEK) at the Albert-Ludwigs-University of Freiburg for the deposition of the polysilicon in the Cleanroom Service Center (RSC). F. Haase and R. Peibst from the Institute for Solar Energy Research Hamelin (ISFH) and J. Krügener from the Institute of Electronic Materials and Devices (MBE) at the University of Hannover are recognized for fruitful discussions within the joint project which was funded by the German Ministry of Economic Affairs and Energy under grant No. 0325827B “26+”.

REFERENCES

[1] P. Cousins, Solar Technology Efficiency: More Breakthroughs are Coming: Solar Technology Efficiency: More Breakthroughs are Coming, 2016.

[2] J. Nakamura, N. Asano, T. Hieda, C. Okamoto, H. Katayama, K. Nakamura, Development of Heterojunction Back Contact Si Solar Cells, IEEE J. Photovoltaics 4 (6) (2014) 1491–1495.

[3] K. Masuko, M. Shigematsu, T. Hashiguchi, D. Fujishima, M. Kai, N. Yoshimura, T. Yamaguchi, Y. Ichihashi, T. Mishima, N. Matsubara, T. Yamanishi, T. Takahama, M. Taguchi, E. Maruyama, S. Okamoto, Achievement of More Than 25% Conversion Efficiency With Crystalline Silicon Heterojunction Solar Cell, IEEE J. Photovoltaics 4 (6) (2014) 1433–1435.

[4] K. Yoshikawa, H. Kawasaki, W. Yoshida, T. Irie, K. Konishi, K. Nakano, T. Uto, D. Adachi, M. Kanematsu, H. Uzu, K. Yamamoto, Silicon heterojunction solar cell with interdigitated back contacts for a photoconversion efficiency over 26%, Nat. Energy 2 (2017) 17032.

[5] M.A. Green, Y. Hishikawa, W. Warta, E.D. Dunlop, D.H. Levi, J. Hohl-Ebinger, A.W. Ho-Baillie, Solar cell efficiency tables (version 50), Prog. Photovolt: Res. Appl. 25 (7) (2017) 668–676.

[6] A. Richter, J. Benick, F. Feldmann, A. Fell, M. Hermle, S.W. Glunz, n-Type Si solar cells with passivating electron contact: Identifying sources for efficiency limitations by wafer thickness and resistivity variation, Solar Energy Materials and Solar Cells (2017).

[7] F. Haase, F. Kiefer, S. Schäfer, C. Kruse, J. Krügener, R. Brendel, R. Peibst, Interdigitated back contact solar cells with polycrystalline silicon on oxide passivating contacts for both polarities, Jpn. J. Appl. Phys. 56 (8S2) (2017) 08MB15.

[8] D. De Ceuster, P. J. Cousins, D. D. Smith Trench process and structure for backside contact solar cells with polysilicon doped regions, 2009.

[9] C. Reichel, F. Feldmann, R. Müller, A. Moldovan, M. Hermle, S.W. Glunz, Interdigitated Back Contact Silicon Solar Cells with Tunnel Oxide Passivated Contacts Formed by Ion Implantation, in: Proceedings of the 29th European Photovoltaic Solar Energy Conference and Exhibition, Amsterdam, The Netherlands, 22-26 September 2014, pp. 487–491.

[10] U. Römer, R. Peibst, T. Ohrdes, B. Lim, J. Krugener, T. Wietler, R. Brendel, Ion Implantation for Poly-Si Passivated Back-Junction Back-Contacted Solar Cells, IEEE J. Photovoltaics 5 (2) (2015) 507–514.

[11] D.L. Young, W. Nemeth, V. LaSalvia, R. Reedy, S. Essig, N. Bateman, P. Stradins, Interdigitated Back Passivated Contact (IBPC) Solar Cells

Formed by Ion Implantation, IEEE J. Photovoltaics 6 (1) (2016) 41–47.

[12] M. Rienäcker, A. Merkle, U. Römer, H. Kohlenberg, J. Krügener, R. Brendel, R. Peibst, Recombination Behavior of Photolithography-free Back Junction Back Contact Solar Cells with Carrier-selective Polysilicon on Oxide Junctions for Both Polarities, Energy Procedia 92 (2016) 412–418.

[13] U. Römer, Dissertation, Gottfried Wilhelm Leibniz Universität Hannover: Polycrystalline silicon / monocrystalline silicon junctions and their application as passivated contacts for Si solar cells. Dissertation, Hannover, 2015.

[14] G. Yang, A. Ingenito, O. Isabella, M. Zeman, IBC c-Si solar cells based on ion-implanted poly-silicon passivating contacts, Solar Energy Materials and Solar Cells 158 (2016) 84–90.

[15] H. Kobayashi Asuha, O. Maida, M. Takahashi, H. Iwasa, Nitric acid oxidation of Si to form ultrathin silicon dioxide layers with a low leakage current density, Journal of Applied Physics 94 (11) (2003) 7328–7335.

[16] F. Feldmann, C. Reichel, R. Müller, M. Hermle, The application of poly-Si/SiOx contacts as passivated top/rear contacts in Si solar cells, Solar Energy Materials and Solar Cells 159 (2017) 265–271.

[17] C. Reichel, F. Feldmann, R. Müller, R.C. Reedy, B.G. Lee, D.L. Young, P. Stradins, M. Hermle, S.W. Glunz, Tunnel oxide passivated contacts formed by ion implantation for applications in silicon solar cells, Journal of Applied Physics 118 (20) (2015) 205701.

[18] F. Feldmann, R. Müller, C. Reichel, M. Hermle, Ion implantation into amorphous Si layers to form carrier-selective contacts for Si solar cells, Phys. Status Solidi RRL 08 (09) (2014) 767–770.

[19] D. Schuldis, A. Richter, J. Benick, P. Saint-Cast, M. Hermle, S.W. Glunz, Properties of the c-Si/Al 2 O 3 interface of ultrathin atomic layer deposited Al 2 O 3 layers capped by SiN x for c-Si surface passivation, Appl. Phys. Lett. 105 (23) (2014) 231601.

[20] S. Lindekugel, H. Lautenschlager, T. Ruof, S. Reber, Plasma hydrogen passivation for crystalline silicon thin-films, in: Proceedings of the 23rd European Photovoltaic Solar Energy Conference (EUPVSEC), Valencia, Spain, 1-5 September 2008, pp. 2232–2235.

[21] J.A. Giesecke, B. Michl, F. Schindler, M.C. Schubert, W. Warta, Minority carrier lifetime of silicon solar cells from quasi-steady-state photoluminescence, Solar Energy Materials and Solar Cells 95 (7) (2011) 1979–1982.

[22] T. Trupke, R.A. Bardos, M.D. Abbott, J.E. Cotter, Suns-photoluminescence: Contactless determination of current-voltage characteristics of silicon wafers, Appl. Phys. Lett. 87 (9) (2005) 93503.

[23] R. A. Sinton, A. Cuevas, M. Stuckings, Quasi-Steady-State Photoconductance, A New Method for Solar Cell Material and Device Characterizatio - Photovoltaic Specialists Conference, 1996., Conference Record of the Twenty Fifth IEEE, in: Proceedings of the 25th IEEE Photovoltaic Specialists Conference (PVSC), Washington D. C., USA, 13-17 May 1996, pp. 457–460.

[24] R.A. Sinton, A. Cuevas, Contactless determination of current–voltage characteristics and minority-carrier lifetimes in semiconductors from quasi-steady-state photoconductance data, Appl. Phys. Lett. 69 (17) (1996) 2510–2512.

[25] D. Pysch, A. Mette, S.W. Glunz, A review and comparison of different methods to determine the series resistance of solar cells, Solar Energy Materials and Solar Cells 91 (18) (2007) 1698–1706.

[26] J. Manoliu, T. I. Kamins, p-n junctions in polycrystalline-silicon films, Solid-State Eleconics (15) (1972) 1103–1106.

[27] M. Dutoit and F. Sollberger, Lateral Polysilicon p-n Diodes, J. Electrochem. Soc. Solid-State Science and Technology 125 (10) (1978) 1648–1651.

[28] N.M. Johnson, D.K. Biegelsen, M.D. Moyer, Grain boundaries in p - n junction diodes fabricated in laser-recrystallized silicon thin films, Appl. Phys. Lett. 38 (11) (1981) 900–902.

[29] R.S. Bonilla, C. Reichel, M. Hermle, P.R. Wilshaw, Extremely low surface recombination in 1 Ω cm n-type monocrystalline silicon, Phys. Status Solidi RRL 11 (1) (2017) 1600307.

[30] M.D. Abbott, R.A. Bardos, T. Trupke, K.C. Fisher, E. Pink, The effect of diffusion-limited lifetime on implied current voltage curves based on photoluminescence data, Journal of Applied Physics 102 (4) (2007) 44502.

[31] T. Trupke, E. Pink, R.A. Bardos, M.D. Abbott, Spatially resolved series resistance of silicon solar cells obtained from luminescence imaging, Appl. Phys. Lett. 90 (9) (2007) 93506.

[32] A. Richter, S.W. Glunz, F. Werner, J. Schmidt, A. Cuevas, Improved quantitative description of Auger recombination in crystalline silicon, Phys. Rev. B 86 (16) (2012) 187.

[33] A. Cuevas, R.A. Sinton, Prediction of the open-circuit voltage of solar cells from the steady-state photoconductance, Prog. Photovolt: Res. Appl. 5 (2) (1997) 79–90.

[34] S.W. Glunz, D. Biro, S. Rein, W. Warta, Field-effect passivation of the SiO2Si interface, Journal of Applied Physics 86 (1) (1999) 683–691.

[35] C. Reichel, R. Müller, F. Feldmann, A. Richter, M. Hermle, S. W. Glunz, submitted for publication (2017).